Computational and Theoretical Chemistry 1091 (2016) 115–121

Contents lists available at ScienceDirect

Computational and Theoretical Chemistry

journal homepage: www.elsevier.com/locate/comptc

DFT study of Li^+ and Na^+ positions in mordenites and hydration stability

Felipe de S. Vilhena [a,*], Ramiro M. Serra [b], Alicia V. Boix [b], Glaucio B. Ferreira [a], José Walkimar de M. Carneiro [a]

[a] Instituto de Química, Universidade Federal Fluminense (UFF), Niterói 24020-141, Brazil
[b] Instituto de Investigaciones en Catálisis y Petroquímica INCAPE (FIQ, UNL-CONICET), Santa Fe, Argentina

ARTICLE INFO

Article history:
Received 11 April 2016
Received in revised form 5 July 2016
Accepted 13 July 2016
Available online 14 July 2016

Keywords:
Periodic calculations
Mordenite
Exchangeable cations
Hydration stability

ABSTRACT

Mordenite is a type of zeolite used in catalysis processes and in the selective adsorption of gases. The properties of this material are related to the presence of aluminium atoms and exchangeable cations in the structure. In this work, we performed DFT periodic calculations of cationic mordenites $X_8Al_8Si_{40}O_{96}$ and $X_4Al_4Si_{44}O_{96}$ ($X = Li^+$ or Na^+) and the corresponding hydrated species. Calculations of Li^+ and Na^+ mordenites indicated preference for the aluminium atoms to occupy T3 and T4 sites. In this configuration, the alkaline cations have preference for the two channels 8MRz and 12MRz along [0 0 1] crystallographic axis. In the hydrated structures, the alkaline cations have preference for the side pockets (8MRy along [0 1 0] direction). Hydrated structures with high aluminium content have a stability caused by interaction of the alkaline cations with water molecules and oxygen atoms of the framework.

1. Introduction

Zeolites are natural or synthetic microporous materials composed by tetrahedral SiO_4 and $(AlO_4)^-$ sites [1]. They are used in a broad range of processes, from gas separation and purification to ion exchange and catalysis [2–5]. The substitution of silicon Si^{4+} for aluminium Al^{3+} introduces a negative charge in the structure, which has to be compensated by the presence of exchangeable ions, such as alkaline and transition metal cations [6].

The Si/Al ratio in zeolites can be controlled experimentally, whereas the exact positions of the aluminium atoms in the framework, and consequently the positions of the exchangeable cations, are much more difficult to be determined [6]. The type of exchangeable ions influences the adsorption or catalytic properties of the zeolites, and their positions are related to the aluminium distribution in the structure. Macroscopically, the localization of the aluminium atoms may vary from the centre of the crystal to the outer edges of the structures. At a microscopic level, it is accepted that two aluminium atoms can never bind to the same oxygen atom, in accordance with the Lowenstein's rule [7].

Mordenite is a type of zeolite used in catalytic processes, such as alkane and olefin cracking, isomerization of hydrocarbons, and in the selective adsorption of gases [8–11]. The framework of mordenites has a one-dimensional channel system, which consists of 12 and 8-membered ring (MR) channels parallel to [0 0 1] crystallographic axis. The main channel (12MRz) has dimensions of about 6.7 × 7.0 Å, while the smaller one (8MRz), in the elliptical shape, has dimensions of 2.6 × 5.7 Å (Fig. 1a). These channels are interconnected along the [0 1 0] direction via 8MRy channel, often referred to as the "side-pockets", formed by a more circular ring (3.4 × 4.8 Å) (Fig. 1b) [12]. Fig. 1c shows the unit cell of silica mordenite that contains 48 silicon and 96 oxygen atoms ($Si_{48}O_{96}$) and encloses 16 T1, 16 T2, 8 T3 and 8 T4 sites. Any of these T sites can be occupied by aluminium atoms, obeying Lowentein's rule [7]. Each aluminium atom introduces a negative charge, which is counterbalanced by the presence of exchangeable cations [13,14]. The type of exchangeable cations and their locations strongly influence the physical and chemical properties of the zeolites [15]. Fig. 1d shows the five possible positions for the exchangeable cations in mordenite, as described in the literature [14,16].

The activity of zeolites arises from substitution of Si^{4+} for Al^{3+} ions [17–19]. This substitution generates an imbalance of negative charge in the structure, which has to be neutralized by a proton or metal cation. The appearance of the positive and negative charges originates the acidic or basic characteristics of the zeolite. Catalytic properties result from cation-framework interactions, allowing the formation of surface complexes as reactive intermediates. The proton associated with oxygen atoms maintains charge neutrality and leads to acidic properties [17,18]. On the other hand, when the negative charge is compensated by cations with low electronegativity, basic properties predominate [18].

The structure of mordenites has been studied by theoretical approaches using both periodic boundary conditions [18–23] and

* Corresponding author.
E-mail address: fs_vilhena@id.uff.br (F. de S. Vilhena).

http://dx.doi.org/10.1016/j.comptc.2016.07.017
2210-271X/

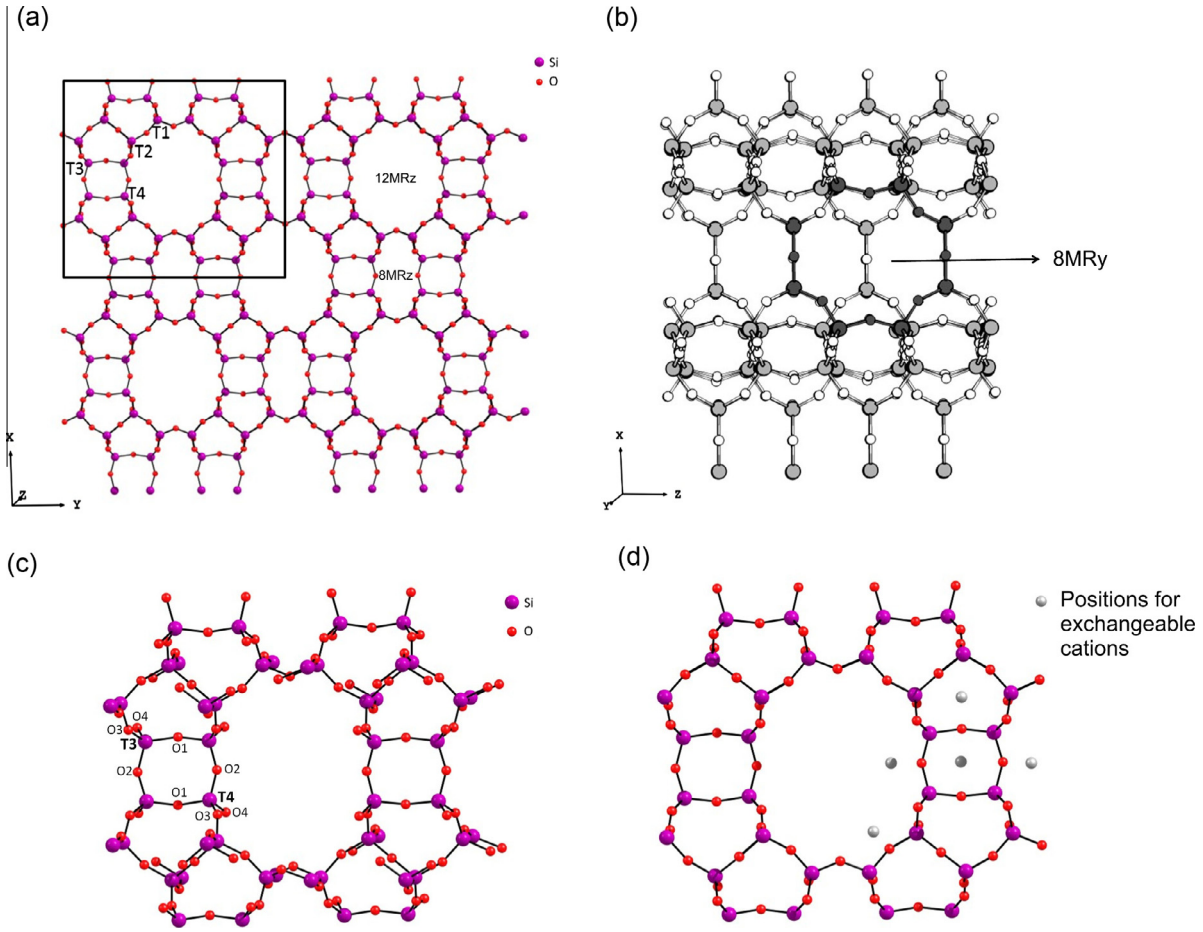

Fig. 1. (a) Periodic representation of mordenite ($2 \times 2 \times 1$) showing the 12MRz and 8MRz channels. The unit cell is delimited by a square; (b) lateral view [0 1 0] of mordenite showing in black the "side pockets" (8MRy); (c) perspective representation of the unit cell of mordenite simulated in the present work, $Si_{48}O_{96}$, and the assignments of tetrahedra and the oxygen atoms in the framework; (d) Five possible positions for the exchangeable cations in the mordenite framework.

extended clusters [16,20,24]. Brönsted acidity, molecular adsorption, IR spectroscopy and hydration effect have been studied with periodic boundary conditions, while the alternative cluster approach has been employed to study local properties such as vibrational frequencies and binding energies. For example, the proton and sodium cation binding energies as well as harmonic vibrational frequencies were computed for a cluster containing 120 tetrahedra enclosing the 12- and 8-membered ring channels [24]. Both periodic and cluster approaches have been shown to yield results in agreement with experiments.

The presence of water molecules in the zeolites influences the distribution and the interaction of the exchangeable cations with the framework [25]. Maurin and co-authors showed that in sodium mordenite, the cations are dislocated from their original positions with the increase in the hydration content [26]. It is known that water molecules coordinate to the cations and increase their mobility across the structure [25,27].

In this work, alkaline mordenites $X_8Al_8Si_{40}O_{96}$ and $X_4Al_4Si_{44}O_{96}$ ($X = Na^+$ and Li^+) and the corresponding hydrated species with eight water molecules were optimized using DFT periodic calculations with the PBE functional and the Ahlrichs VDZ basis set. The preferential positions for aluminium atoms and the influence of water molecules in the exchangeable cation positions were explored.

2. Computational methods

Atomic coordinates and unit cell parameters of a sodium hydrated crystalline mordenite structure were taken from the International Zeolite Association (IZA) site [28]. The downloaded sodium hydrated mordenite structure contains 24 water molecules. Some of the hydration water showed no specific interaction with the modernite framework or the cations, and therefore they were excluded from our model, which preserved only the eight water molecules directly coordinated to/or surrounding the sodium cations. Two Si/Al ratios were explored, 5 and 11. The aluminium atoms were placed in the T sites, obeying Lowentein's rule [7]. The Li^+ and Na^+ cations were conserved in their original positions in the channels and the structures were then fully optimized. The optimizations of $Si_{48}O_{96}$, $Si_{48}O_{96}{\cdot}8H_2O$, $X_8Al_8Si_{40}O_{96}$, $X_8Al_8Si_{40}O_{96}{\cdot}8H_2O$, $X_4Al_4Si_{44}O_{96}$ and $X_4Al_4Si_{44}O_{96}{\cdot}8H_2O$ ($X = Li^+$ and Na^+) structures were performed by means of DFT periodic calculations using the CP2 K program [29] with the cell parameters $a = 18.256$; $b = 20.534$; $c = 7.542$ Å and $\alpha = \beta = \gamma = 90°$. The calculations were carried out using the mixed Gaussian and plane-wave (GPW) method [30–32] and PBE exchange-correlation functional [33] with VDZ Valence Double Zeta (Ahlrichs VDZ) basis set [34]. The density cutoff of 500 a.u and the dimensional periodic condition of $1 \times 1 \times 1$ were used.

3. Results and discussion

3.1. Dehydrated $X_8Al_8Si_{40}O_{96}$ (Si/Al = 5) and $X_4Al_4Si_{44}O_{96}$ (Si/Al = 11) mordenites ($X = Li^+$ or Na^+)

In the mordenite framework, the aluminium atoms could occupy T1, T2, T3 or T4 sites. For $Li_8Al_8Si_{40}O_{96}$ (Li-MOR) and

Table 1
Relative energies (kcal mol^{-1}) for the possible positions of the aluminium atoms in $Li_8Al_8Si_{40}O_{96}$ and $Na_8Al_8Si_{40}O_{96}$ (Si/Al = 5), computed with the PBE functional and the Ahlrichs VDZ basis set.

Al sitting in T sites	Li-MOR	Na-MOR
T3—O—Si—O—T4	0	0
T3—O—Si—O—T2	59.3	50.1
T4—O—(Si—O)$_2$—T1	93.2	87.4

$Na_8Al_8Si_{40}O_{96}$ (Na-MOR) structures, three configurations for aluminium atoms in the T sites were tested: T3—O—Si—O—T4, T3—O—Si—O—T2 and T4—O—(Si—O)$_2$—T1 (see Fig. 1a). Although it has been suggested that the aluminium positions are controlled by experimental conditions [6], our theoretical calculations show a clear preference for the T3—O—Si—O—T4 configuration (Table 1), in agreement with previous computations using *ab initio* molecular

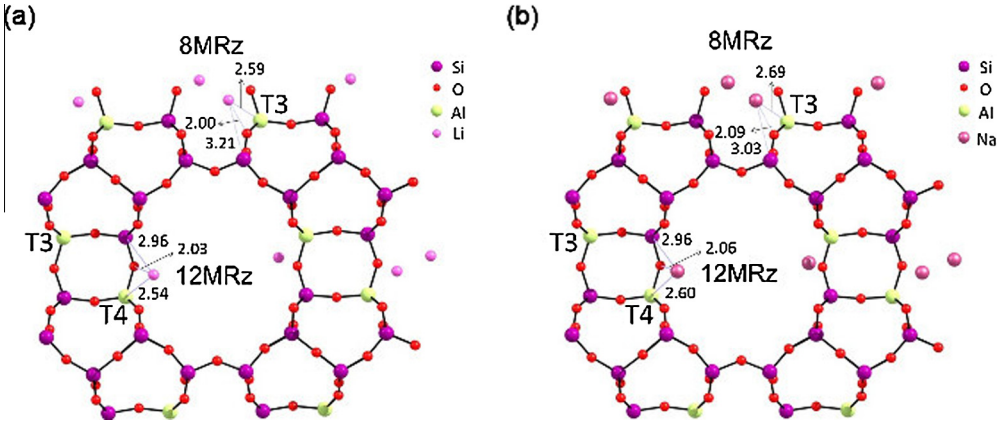

Fig. 2. DFT periodic optimized structures of alkaline mordenites with high aluminium content (Si/Al = 5). (a) $Li_8Al_8Si_{40}O_{96}$ with aluminium atoms in the T3 and T4 sites; (b) $Na_8Al_8Si_{40}O_{96}$ with aluminium atoms in the T3 and T4 sites. Computed with the PBE functional and the Ahlrichs VDZ basis set.

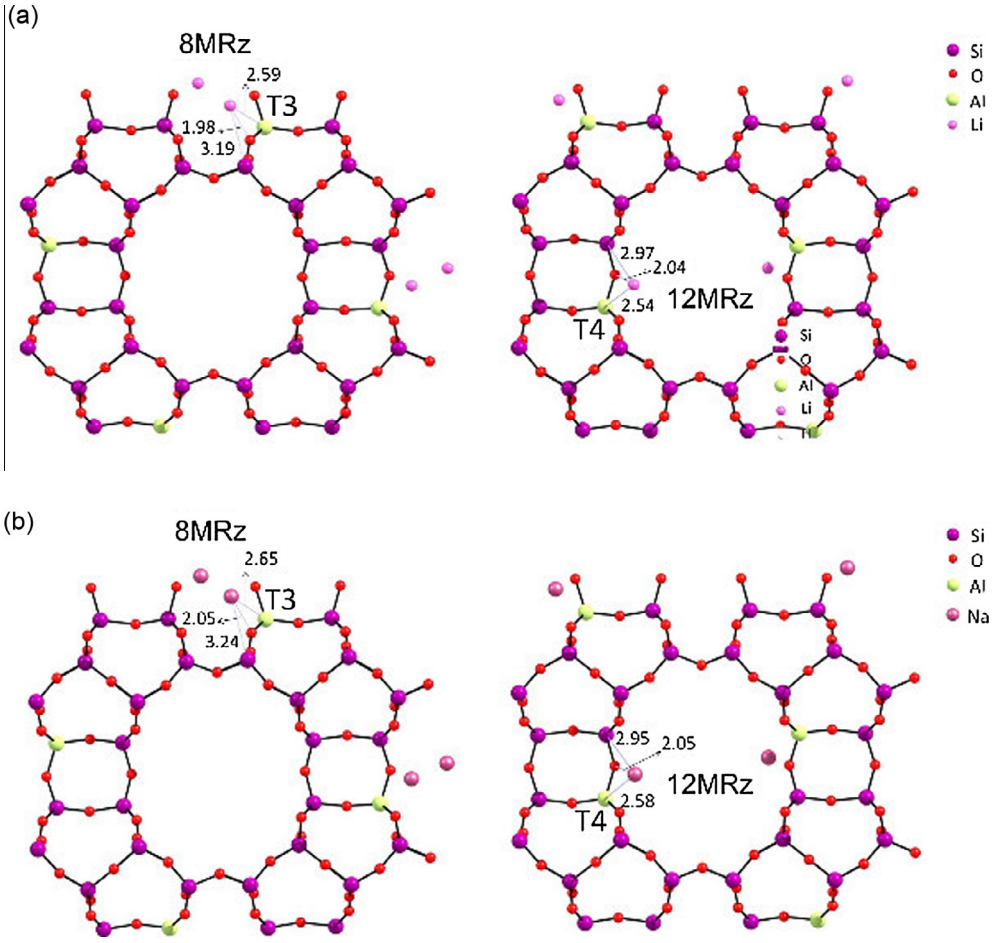

Fig. 3. DFT periodic optimized structures of alkaline mordenites with low aluminium content (Si/Al = 11). (a) $Li_4Al_4Si_{44}O_{96}$ with aluminium atoms in the T3 or in the T4 site and (b) $Na_4Al_4Si_{44}O_{96}$ with aluminium atoms in the T3 or in the T4 site. Bond lengths in Å. Computed with the PBE functional and Ahlrichs the VDZ basis set.

calculations [19,24,35], which reported a higher stability of the T3 and T4 sites.

The distribution of aluminium atoms in the structure of natural and synthetic mordenite has been determined by crystallographic experiments [35,36]. For a natural mordenite, aluminium was found to preferentially occupy the T3 position, followed by the T4 site [35]. Similarly, a study based on expanded clusters has found the T3 and T4 sites as the preferential for the aluminium sitting positions [24]. Based on these findings, and assuming the results shown in Table 1, which also indicate a preference for the T3 and T4 sites in our periodic model, our further calculations were performed with aluminium atoms occupying the T3 and T4 sites.

Table 2
Selected optimized geometrical parameters and Mulliken atomic charges of mordenites $Li_8Al_8Si_{40}O_{96}$, $Na_8Al_8Si_{40}O_{96}$, $Li_4Al_4Si_{44}O_{96}$ and $Na_4Al_4Si_{44}O_{96}$ computed with the PBE functional and the Ahlrichs VDZ basis set. Distances in Angstroms (Å).

Bond distances	Li-MOR Si/Al = 5	Na-MOR Si/Al = 5	Li-MOR[a] Si/Al = 11	Na-MOR[a] Si/Al = 11
T3—O1	1.64	1.65	1.64	1.64
T3—O2	1.68	1.68	1.68	1.67
T3—O3	1.72	1.72	1.72	1.72
T3—O4	1.65	1.66	1.65	1.65
T4—O1	1.62	1.64		
T4—O2	1.63	1.63		
T4—O3	1.59	1.59		
T4—O4	1.67	1.66		
Charges(e)				
T3	1.98	2.01	1.98	2.00
O1	−1.27	−1.26	−1.27	−1.26
O2	−1.31	−1.32	−1.31	−1.32
O3	−1.30	−1.30	−1.31	−1.31
O4	−1.22	−1.21	−1.22	−1.22
$(T3O_4)^-$	−0.57	−0.54	−0.58	−0.55
X[b]	0.85	0.83	0.85	0.83
[X[b](T3O4)]	0.28	0.29	0.27	0.28
T4	2.07[b]	2.06		
O1	−1.34	−1.21		
O2	−1.26	−1.24		
O3	−1.23	−1.24		
O4	−1.33	−1.22		
$(T4O_4)^-$	−0.51	−0.40		
X[c]	0.93	0.87		
[X[c](T4O4)]	0.42	0.47		

[a] Al atoms in the T3 site.
[b] Alkaline cations in the 8MRz channel.
[c] Alkaline cations in the main channel (12MRz).

Using this configuration, we investigated the positions of the alkaline cations. In the $Li_8Al_8Si_{40}O_{96}$ and $Na_8Al_8Si_{40}O_{96}$ optimized structures, the alkaline cations prefer to be located in the 8MRz and 12MRz channels (Fig. 2), showing that the exchangeable cations are preferentially located close to the aluminium atoms, a result in line with those of Maurin and coauthors, who found that in dehydrated Na-mordenite the sodium atoms are located in the two channels [26]. In the $Li_8Al_8Si_{40}O_{96}$ structure, the distances from the Li^+ to the oxygen atom (O2) in 8MRz and 12MRz are 2.00 and 2.03 Å, respectively, smaller than the corresponding distances in $Na_8Al_8Si_{40}O_{96}$, which are 2.09 and 2.06 Å (Fig. 3). The smaller ionic radius of Li^+ (90 pm) causes a stronger electrostatic interaction with the oxygen atoms in the framework, reflected in the smaller Li—O bond distances. The geometrical parameters (Table 2) are in a good agreement with experimental data [35] and theoretical studies using cluster approach for sodium mordenite [24].

The structures with lower aluminium content, Si/Al ratio equal to 11, were explored with the aluminium atoms sitting in the T3 or in the T4 sites (Fig. 3). The DFT periodic calculations for $Li_4Al_4Si_{44}O_{96}$ (Li-MOR) and $Na_4Al_4Si_{44}O_{96}$ (Na-MOR) indicated the preference of the Al atoms for the T3 site rather than for T4, by 27.1 and 30.9 kcal mol^{-1}, respectively. In general, our results agree with a reported crystal structure refinement, which indicated that for mordenites with different Si/Al ratios, the Al site preference follows the order T3 > T4 > T1 > T2 [35,36], and with results employing cluster approach for sodium mordenite, which indicated the preference for the T3 rather than for the T4 site [24].

Table 2 shows the bond lengths and the Mulliken atomic charges for $X_8Al_8Si_{40}O_{96}$ and $X_4Al_4Si_{44}O_{96}$ (Al in the T3 site) structures (X = Li^+ or Na^+). The charges of the $(TO_4)^-$ group were obtained as the sum of the charge of the T atom (aluminium or silicon) plus the charge of the four oxygen atoms divided by two (considering that each oxygen atom participates in two $(TO_4)^-$ groups). For the charge on the [X(TO_4)] group, we added the positive charge of the X atom (X = Li^+ or Na^+). The total charges of the $(TO_4)^-$ and [X(TO_4)] groups give an indication of the basic or acidic properties of the mordenites, respectively [20]. In the $Li_8Al_8Si_{40}O_{96}$ and $Na_8Al_8Si_{40}O_{96}$ structures, the total negative charges of $(T3O_4)^-$ and $(T4O_4)^-$ are similar (Table 2). However, the positive charges on the [X($T4O_4$)] group of +0.42 and +0.47*e*, respectively, are higher than those in the [X($T3O_4$)] group (+0.28 and +0.29*e*). These results suggest that in the adsorption process on mordenites with high aluminium content (Si/Al = 5), the basic centre of an adsorbed

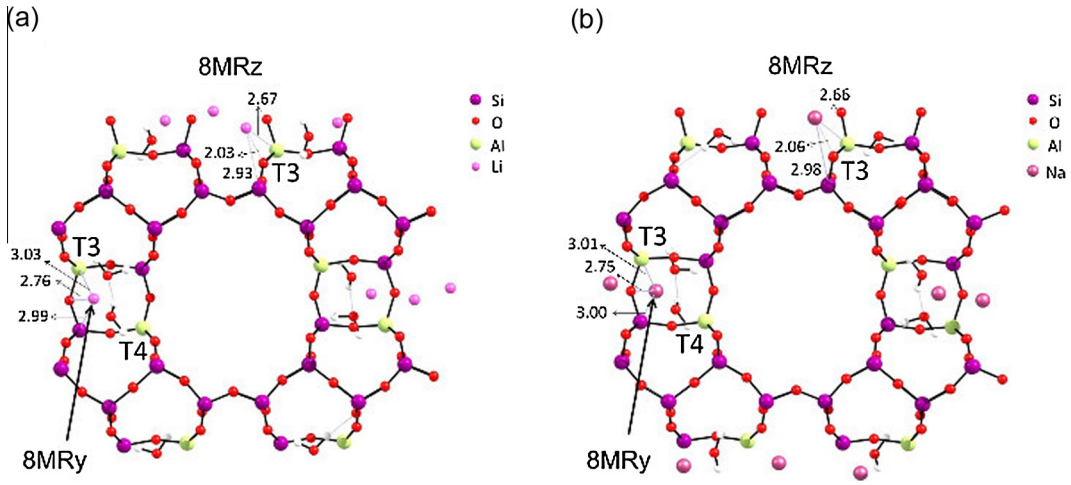

Fig. 4. DFT optimized structures of Li^+ and Na^+ hydrated mordenites with Si/Al ratio of 5. (a) $Li_8Al_8Si_{40}O_{96}{\cdot}8H_2O$ and (b) $Na_8Al_8Si_{40}O_{96}{\cdot}8H_2O$. Bond lengths in Å. Computed with the PBE functional and the Ahlrichs VDZ basis set.

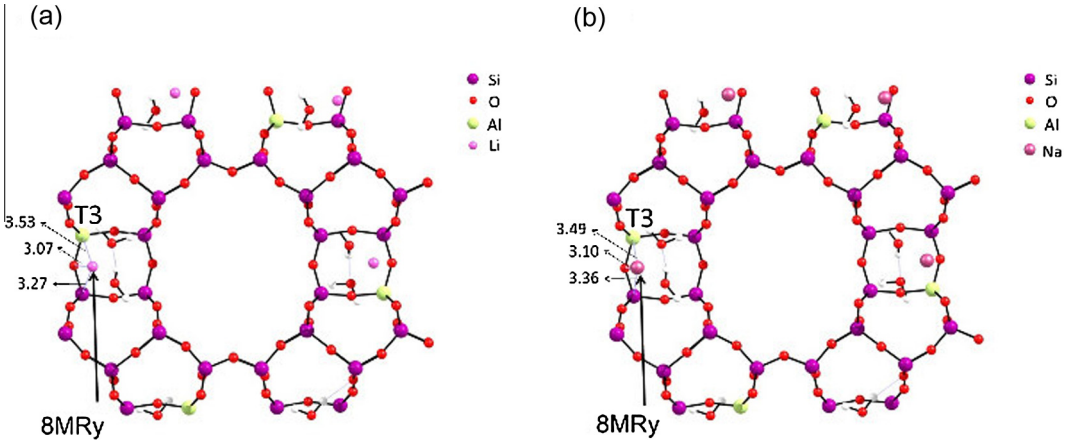

Fig. 5. DFT optimized structures of hydrated mordenites with Si/Al ratio of 11. (a) $Li_4Al_4Si_{44}O_{96}{\cdot}8H_2O$ and (b) $Na_4Al_4Si_{44}O_{96}{\cdot}8H_2O$. Bond lengths in Å. Computed with the PBE functional and the Ahlrichs VDZ basis set.

molecule prefer to interact with the 12MRz channel, closer to the [X(T4O$_4$)] site (with higher positive charge) than with the 8MRz channel, in which the [X(T3O$_4$)] site has lower positive charge. In the structures with Si/Al ratios of 5 and 11, the distances from the alkaline cation to the framework atoms, as well as the Mulliken atomic charges, are similar, indicating that changing the amount of aluminium atoms does not affect the interaction of the exchangeable cations with the framework.

In the Li^+ and Na^+ mordenite frameworks (Si/Al = 5), the preferential positions for the aluminium atoms are the T3 and T4 sites, in the closest distance between each other, obeying the Lowenstein's rule [7]. In the T3—O—Si—O—T4 configuration, the Li^+ and Na^+ cations occupy the 12MRz and 8MRz channels, close to the aluminium atoms. The acidic X[(T4O$_4$)] group shows a higher positive charge than the [X(T3O$_4$)] one (X = Li^+ or Na^+), indicating that the [X(T4O$_4$)] group has stronger attraction for a basic adsorbate. In the structures with low aluminium content (Si/Al = 11), the aluminium atoms prefer the 8MRz channel rather than the larger one (12MRz). In these structures, the interactions of exchangeable cations with oxygen atoms of the framework are similar to those found in the structures with high aluminium concentration.

3.2. Hydrated $X_8Al_8Si_{40}O_{96}{\cdot}8H_2O$ (Si/Al = 5) and $X_4Al_4Si_{44}O_{96}{\cdot}8H_2O$ (Si/Al = 11) mordenites (X = Li^+ or Na^+)

From the crystallographic structure of mordenite, excluding those water molecules not directly coordinated to the alkaline cations, and assuming the preferential positions for the aluminium atoms as discussed above (structure shown in Fig. 2, Si/Al = 5), we obtained hydrated structures containing eight water molecules located in the side pockets (8MRy). These hydrated structures were optimized to identify the preferential positions for the alkaline cations. Two set of positions for the alkaline cations were tested, one with the cations located in the 8MRz and in the 12MRz channels, and another with the cations placed in the 8MRz and in the side pocket (8MRy) channels. In the $Li_8Al_8Si_{40}O_{96}{\cdot}8H_2O$ (Li-MOR·8H$_2$O) and $Na_8Al_8Si_{40}O_{96}{\cdot}8H_2O$ (Na-MOR·8H$_2$O) structures, the configuration with the alkaline cations located in the 8MRz and 8MRy positions (Fig. 4) shows a higher stability, by −36.5 and −27.9 kcal mol^{-1}, respectively, than that in which the cations occupy the 8MRz and 12MRz positions. Our results indicate that the alkaline cations, upon optimization in the presence of a few water molecules, move from their initial positions (12MRz) to the side pockets (8MRy) [26]. The X-Si, X-O and X-Al (X = Li^+ and Na^+) bond distances in the Li-MOR·8H$_2$O and Na-MOR·8H$_2$O structures (Si/Al = 5) are essentially the same. However, the X—O distances in the side pockets (8MRy) are greater than that in the smaller channel (8MRz). In the side pockets (8MRy), the alkaline cations are surrounded by water molecules, and this interaction increases the distances to the oxygen atoms (O2) of the framework (Fig. 4).

The hydrated structures with Si/Al ratio of 11 were optimized with the alkaline cations located in the 8MRz or in the 8MRy channels. The Li-MOR·8H$_2$O and Na-MOR·8H$_2$O structures with the alkaline cations located in the side pockets (8MRy) (Fig. 5) show higher stability, by −55.8 and −62.3 kcal mol^{-1}, respectively, than the structures with the alkaline cations placed in the smaller channel (8MRz). The preference for the side pocket is the same as that observed in the hydrated structures with the higher aluminium

Table 3
Selected optimized geometrical parameters and Mulliken atomic charges of hydrated mordenites $X_8Al_8Si_{40}O_{96}{\cdot}8H_2O$ and $X_4Al_4Si_{44}O_{96}{\cdot}8H_2O$ (X = Li^+ or Na^+). Computed with the PBE functional and the Ahlrichs VDZ basis set.

Bond distances	Li-MOR·8H$_2$O Si/Al = 5	Na-MOR·8H$_2$O Si/Al = 5	Li-MOR·8H$_2$O[a] Si/Al = 11	Na-MOR·8H$_2$O[a] Si/Al = 11
T3—O1	1.71	1.64	1.70	1.70
T3—O2	1.62	1.71	1.65	1.65
T3—O3	1.67	1.69	1.67	1.67
T3—O4	1.67	1.67	1.68	1.69
T4—O1	1.69	1.69		
T4—O2	1.59	1.59		
T4—O3	1.61	1.62		
T4—O4	1.61	1.61		
Charges (e)				
T3	1.91	1.93	1.96	1.96
O1	−1.26	−1.27	−1.24	−1.24
O2	−1.32	−1.26	−1.21	−1.22
O3	−1.23	−1.32	−1.22	−1.22
O4	−1.32	−1.32	−1.21	−1.22
(T3O$_4$)$^-$	−0.66	−0.66	−0.48	−0.49
T4	2.09	2.10		
O1	−1.21	−1.22		
O2	−1.26	−1.26		
O3	−1.23	−1.23		
O4	−1.23	−1.23		
(T4O$_4$)$^-$	−0.37	−0.37		
X[b]	0.66	0.68	–	–
[X[b](T3O$_4$)]	0.00	0.02	–	–
X[c]	0.79	0.80	0.72	0.73
[X[c](T3O$_4$)]	0.13	0.14	0.24	0.24

[a] Al atoms in the T3 site.
[b] Alkaline cations in the 8MRz channel.
[c] Alkaline cations in the side pockets (8MRy).

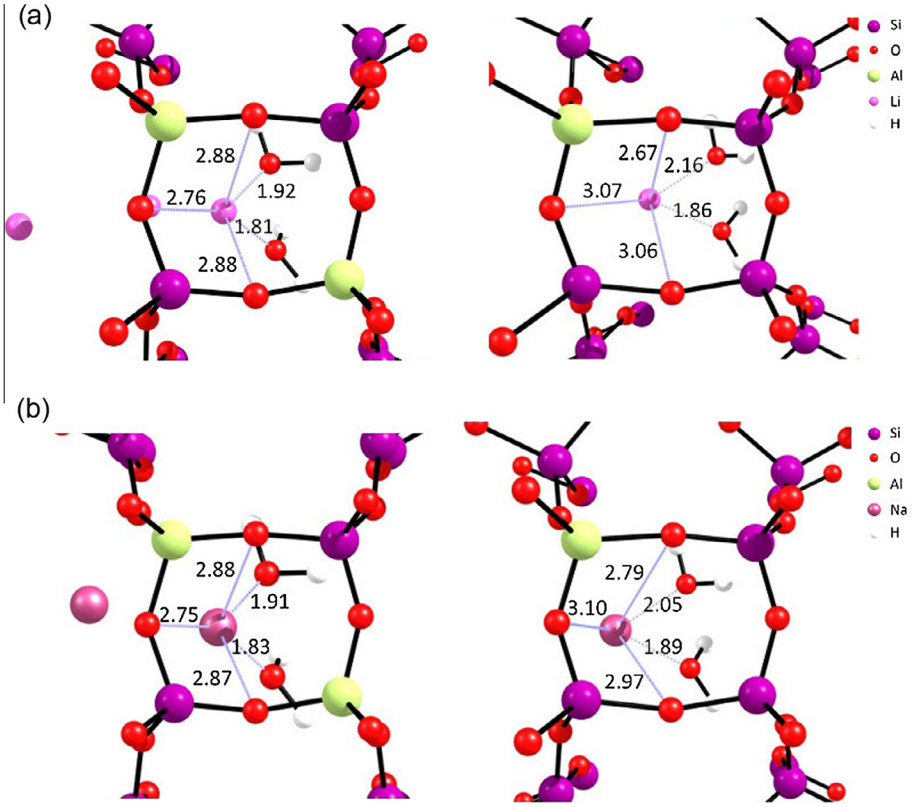

Fig. 6. Coordination sphere of Li^+ and Na^+ located in the side pockets (8MRy) in the hydrated mordenites with Si/Al ratios of 5 and 11. (a) $Li_8Al_8Si_{40}O_{96}{\cdot}8H_2O$ and $Li_4Al_4Si_{44}O_{96}{\cdot}8H_2O$. (b) $Na_8Al_8Si_{40}O_{96}{\cdot}8H_2O$ and $Na_4Al_4Si_{44}O_{96}{\cdot}8H_2O$. Bond lengths in Å. Computed with the PBE functional and the Ahlrichs VDZ basis set.

content (Si/Al = 5). However, in this case (hydrated structures, Si/Al = 11), the preference for the 8MRy site, as compared to the 8MRz channel, is higher.

Table 3 shows the bond lengths and the Mulliken atomic charges for the $X_8Al_8Si_{40}O_{96}{\cdot}8H_2O$ and $X_4Al_4Si_{44}O_{96}{\cdot}8H_2O$ structures (X = Li^+ or Na^+). Fig. 6 presents the metal coordination sphere of Li^+ and Na^+ in the side pockets (8MRy) of the hydrated structures with the two Si/Al ratios studied (5 and 11). The alkaline cations bind to two oxygen atoms of two water molecules and three oxygen atoms of the framework, presenting a pentacoordinated sphere (considering coordination for distances below 3.0 Å). The positive charges on the [$X^c(T3O_4)$] group (X = Li^+ or Na^+, X^c cations in the side pockets) are greater in the hydrated structures with Si/Al of 11 (+0.24*e*) than in the hydrated structures with Si/Al ratio of 5 (+0.13 and +0.14*e*, respectively) (Table 3).

Table 4
Energy difference (kcal mol^{-1}) between the hydrated Li^+ and Na^+ mordenites and the corresponding dehydrated structures with Si/Al ratios of 5 and 11. Computed with the PBE functional and the Ahlrichs VDZ basis set.

Comparison	Energy difference	Energy contribution by one water molecule[a]
$Si_{48}O_{96}{\cdot}8H_2O$ - [$Si_{48}O_{96}$ + $8H_2O$]	−81.2	−10.1
$Li_8Al_8Si_{40}O_{96}{\cdot}8H_2O$ - [$Li_8Al_8Si_{40}O_{96}$ + $8H_2O$]	−359.3	−44.9
$Na_8Al_8Si_{40}O_{96}{\cdot}8H_2O$ - [$Na_8Al_8Si_{40}O_{96}$ + $8H_2O$]	−347.5	−43.4
$Li_4Al_4Si_{44}O_{96}{\cdot}8H_2O$ - [$Li_4Al_4Si_{44}O_{96}$ + $8H_2O$]	−310.4	−38.8
$Na_4Al_4Si_{44}O_{96}{\cdot}8H_2O$ - [$Na_4Al_4Si_{44}O_{96}$ + $8H_2O$]	−307.6	−38.4

[a] Energy difference divided by eight (kcal mol^{-1}), describing the interaction energy of each water molecule.

3.3. Hydration stability

We computed the energy difference between the hydrated structures and the corresponding dehydrated ones, plus the energy of the eight adsorbed water molecules to quantify the stability due to hydration (Table 4). This gives an average value for the interaction energy of the water molecules with the framework. As eight water molecules are present in the structures, the interaction energies due to each water molecule in $Si_{48}O_{96}{\cdot}8H_2O$, $Li_8Al_8Si_{40}O_{96}{\cdot}8H_2O$ and $Na_8Al_8Si_{40}O_{96}{\cdot}8H_2O$ (Si/Al = 5) are −10.1, −44.9 and −43.4 kcal mol^{-1}, respectively. For the structures $Li_4Al_4Si_{44}O_{96}{\cdot}8H_2O$ and $Na_4Al_4Si_{44}O_{96}{\cdot}8H_2O$ (Si/Al = 11) the interaction energies are −38.8 and −38.4 kcal mol^{-1}, respectively.

The presence of the metal cations increases the interaction of the water molecule with the framework, and the interaction is slightly stronger for Li-MOR·$8H_2O$ than for Na-MOR·$8H_2O$.

Regarding the effect of the aluminium content on the interaction with the water molecules, it can be seen that structures with higher aluminium content results in stronger interaction with the water molecules.

Only the metal cations in the side pockets (8MRy) are surrounded by water molecules, with each one coordinated to two water molecules. Therefore, the interaction in each case is of the same nature. The M^+-OH_2 distances in the structures with the higher aluminium content are smaller than the corresponding distances in the structures with lower aluminium content. Also, the average M^+-O (oxygen atoms of the framework) distance is smaller in the structures with higher aluminium content. Thus, the higher stability of the structures with higher aluminium content is due to the interactions of the alkaline cations with water molecules and oxygen atoms of the framework.

4. Conclusions

Our results based on periodic calculations indicate that the preferential sites for the aluminium atoms in mordenite with a Si/Al ratio of 5 are the T3 and T4 positions. For the dehydrated mordenites with this Si/Al ratio, the alkaline Li^+ and Na^+ cations prefer to be located in the 12MRz and 8MRz channels. When reducing the aluminium content, the T3 site becomes preferential and the cations are found in the 8MRz channel.

In the presence of water molecules in the structures, the alkaline cations migrate from the 12MRz channel to the side pockets, where they become solvated by the water molecules. In the Li^+ and Na^+ hydrated mordenites, a higher stability of the structures with higher aluminium content is due to the interactions between the alkaline cations with the water molecules and oxygen atoms of the framework.

Acknowledgements

This research was supported by a grant from the Brazilian agency CAPES (PNPD program) and the Bilateral Cooperation Project FAPERJ-CONICET (Grant Number E-26/110.041/2014).

References

[1] J. Cejka, A. Corma, S. Zones (Eds.), Zeolites and catalysis: synthesis, Reactions and Applications, Wiley-VCH, Weinheim, 2010.
[2] M. Stöcker, Gas phase catalysis by zeolites, Micropor. Mesopor. Mater. 82 (2005) 257–292.
[3] A. Dyer, A.P. Singh, Effect of cation exchange on heat of sorption and catalytic activity of mordenites, Zeolites 8 (1988) 242–246.
[4] M.C. Silaghi, C. Chizallet, E. Petracovschi, T. Kerber, J. Sauer, P. Raybaud, Regioselectivity of Al–O Bond hydrolysis during zeolites dealumination unified by Brønsted-Evans-Polanyi relationship, ACS Catal. 5 (2015) 11–15.
[5] J.A. Rabo, M.W. Schoonover, Early discoveries in zeolite chemistry and catalysis at union carbide, and follow-up in industrial catalysis, Appl. Catal. A 222 (2001) 261–275.
[6] J. Dedecek, Z. Sobalik, B. Wichterlova, Siting and distribution of framework aluminium atoms in silicon-rich zeolites and impact on catalysis, Catal. Rev. 54 (2012) 135–223.
[7] W. Löewenstein, The distribution of aluminum in the tetrahedra of silicates and aluminates, Am. Miner. 39 (1954) 92–96.
[8] G.L. Zhao, J.W. Teng, Z.K. Xie, W.M. Yang, Q.L. Chen, Y. Tang, Catalytic cracking reactions of C4-olefin over zeolites H-ZSM-5, H-mordenite and H-SAPO-34, Stud. Surf. Sci. Catal. 170 (2007) 1307–1312.
[9] R.J. Davis, Aromatization on zeolite L - supported Pt clusters, Het. Chem. Rev. 1 (1994) 41–53.
[10] A. Thijs, G. Peeters, E.F. Vansant, I. Verhae, Purification of gases in H-mordenite modified with silane and diborane, J. Chem. Soc., Faraday Trans. 1 (79) (1983) 2821–2834.
[11] C.E. Webster, A. Cottone, S. Drago, Multiple equilibrium analysis description of adsorption on Na-mordenite and H-mordenite, J. Am. Chem. Soc. 121 (1999) 12127–12139.
[12] A. Alberti, P. Davoli, G. Vezzalini, The crystal structure refinement of a natural mordenite, Z. Kristallogr. 175 (1986) 249–256.
[13] D.W. Ming, J.B. Dixon, Quantitative determination of clinoptilolite in soils by a cation-exchange capacity method, Clays Clay Miner. 35 (1987) 463–468.
[14] W. Mortier, Compilation of Extra Framework Sites in Zeolites, Butterworths Sci. Ltd, Guilord, 1982.
[15] J.M. Kalegoras, .A. Vassilikou-Dova, Defect and Diffusion Forum, in: D.J. Fisher (Ed.), SCITEC Publication, New York, 1998.
[16] K. Sun, W. Su, F. Fan, Z. Feng, T.A.P.J. Jansen, R.A. van Santen, C. Li, Location of Mg cations in mordenite zeolite studied by IR spectroscopy and density functional theory simulations with a CO adsorption probe, J. Phys. Chem. A 112 (2008) 1352–1358.
[17] S.R. Stoyanov, S. Gusarov, S.M. Kuznicki, A. Kovalenko, Theoretical modeling of zeolite nanoparticle surface acidity for heavy oil upgrading, J. Phys. Chem. C 112 (2008) 6794–6810.
[18] S. Sklenak, P.C. Andrikopoulos, S.R. Whittleton, H. Jirglova, P. Sazama, L. Benco, T. Bucko, J. Hafner, Z. Sobalik, Effect of the Al siting on the structure of Co(II) and Cu(II) cationic sites in ferrierite. A periodic DFT molecular dynamics and FTIR study, J. Phys. Chem. C 117 (2013) 3958–3968.
[19] T. Demuth, J. Hafner, L. Benco, H. Toulhoat, Structural and acidic properties of mordenite. An ab initio density-functional study, J. Phys. Chem. B 104 (2000) 4593–4607.
[20] G. Sastre, N. Katada, M. Niwa, Computational study of Brønsted acidity of mordenite. Effect of the electric field on the infrared OH stretching frequencies, J. Phys. Chem. C 114 (2010) 15424–15431.
[21] R. Grybos, J. Hafner, L. Benco, P. Raybaud, Adsorption of NO on Pd-exchanged mordenite: ab initio DFT modeling, J. Phys. Chem. C 112 (2008) 12349–12362.
[22] L. Benco, T. Bucko, J. Hafner, H. Toulhoat, A density functional theory study of molecular and dissociative adsorption of H_2 on active sites in mordenite, J. Phys. Chem. B 109 (2005) 22491–22501.
[23] L. Benco, D. Tunega, Adsorption of H_2O, NH_3 and C_6H_6 on alkali metal cations in internal surface of mordenite and in external surface of smectite: a DFT study, Phys. Chem. Miner. 36 (2009) 281–290.
[24] V.D. Dominguez-Soria, P. Calaminici, Theoretical study of the structure and properties of Na-MOR and H-MOR zeolite models, J. Chem. Phys. 127 (2007) 154710–154718.
[25] P. Pissis, D. Daoukaki-Diamanti, Dielectric studies of molecular mobility in hydrated zeolites, J. Phys. Chem. Solids 54 (1993) 701–709.
[26] G. Maurin, R.G. Bell, S. Devautour, F. Henn, J.C. Giuntini, Modeling the effect of hydration in zeolite Na^+-mordenite, J. Phys. Chem. B 108 (2004) 3739–3745.
[27] G. Artioli, J.V. Smith, A. Kvick, J.J. Pluth, K. Stahl, in: B. Dram, S. Hocevar, S. Paovnik (Eds.), Zeolites, Elsevier, Amsterdam, 1985.
[28] C. Baerlocker, L.B. McCusker, Database of Zeolite Structures, ETH Zurich, International Zeolite Association, Framework Structure Database.
[29] The CP2K Developers Group. CP2K Open Source Molecular Dynamics Program, <http://www.CP2K.org/>.
[30] V.J. Vande, M. Krack, F. Mohamed, M. Parrinello, T. Chassaing, J. Hutter, Quickstep: fast and accurate density functional calculations using a mixed Gaussian and plane waves approach, Comput. Phys. Commun. 167 (2005) 103–128.
[31] P.E. Blochl, Projector augmented-wave method, Phys. Rev. B 50 (1994) 17953–17979.
[32] P.E. Blochl, C.J. Forst, J. Schimpl, The projector augmented wave method: ab-initio molecular dynamics with full wave functions, Bull. Mater. Sci. 26 (2003) 33–41.
[33] J.P. Perdew, K. Burke, M. Ernzerhof, Generalized gradient approximation made simple, Phys. Rev. Lett. 77 (1996) 3865–3868.
[34] A. Schafer, H. Horn, R. Ahlrichs, Fully optimized contracted gaussian basis sets for atoms Li to Kr, J. Chem. Phys. 97 (1992) 2571–2577.
[35] P. Simoncic, T. Armbruster, Peculiarity and defect structure of the natural and synthetic zeolite mordenite: a single-crystal X-ray study, Am. Miner. 89 (2004) 421–431.
[36] A. Alberti, Location of Brönsted sites in mordenite, Zeolites 19 (1997) 411–415.